LIESST Effect Studies of Iron(II) Spin-Crossover Complexes with Phosphine Ligands: Relaxation Kinetics and Effects of Solvent Molecules

Chi-Cheng Wu,[1] Jürgen Jung,[2] Peter K. Gantzel,[1] Philipp Gütlich,*[,2] and David N. Hendrickson*[,1]

Department of Chemistry and Biochemistry 0358, University of California at San Diego, La Jolla, California 92093-0358, and Institut für Anorganische Chemie und Analytische Chemie, Johannes Gutenberg Universität, D-55099 Mainz, Germany

Received January 10, 1997[⊗]

^{57}Fe Mössbauer data are presented to show that polycrystalline samples of $[Fe(dppen)_2X_2]\cdot 2S$, where dppen is cis-1,2-bis(diphenylphosphino)ethylene and X^- is Cl^- or Br^- and S is $CHCl_3$ or CH_2Cl_2, exhibit the light-induced excited spin state trapping (LIESST) effect. If the sample is kept at 10 K, Ar ion laser light converts the whole sample from the thermally stable low-spin (LS) form to the metastable high-spin (HS) form, while light of $\lambda >$ 695 nm converts some of the metastable HS to the stable LS form. The relaxation rate was monitored in the 28−70 K range following the LIESST effect at 10 K. The plots of the fraction of HS complex (γ_{HS}) *vs* time can be fitted reasonably well to a single exponential for the four complexes. The relaxation data were also analyzed with a model for cooperative (γ_{HS}-dependent decay) relaxation. It is found that complex **1** shows less cooperativity than the other three complexes. Furthermore, the HS → LS relaxation times observed in the ∼28−70 K range for these four complexes are relatively long compared with those for FeN_6 complexes under similar conditions. The relaxation kinetics of $[Fe(dppen)_2Cl_2]\cdot n CHCl_3$ (**1**) appears to be affected by the amount (n) of solvent molecules in the crystal lattice. Variable-temperature magnetic susceptibility data show that only when each complex has fully two solvent molecules does the conversion from HS at high temperatures to LS at low temperatures go to completion. The results of the X-ray structures of $[Fe(dppen)_2Br_2]\cdot 2CHCl_3$ (**3**) at 149 and 193 K are given, *i.e.*, below and above the LS to HS ($T_{1/2} = 175$ K) conversion. At both temperatures, complex **3** has the monoclinic space group $P2_1/c$, which at 149 K has a unit cell with $a = 11.494(16)$ Å, $b = 12.895(14)$ Å, $c = 17.49(2)$ Å, and $Z = 2$. Refinement of the 149 K data set with 3434 observed [$F_o > 4\sigma(F_o)$] reflections gave $R = 0.0816$ and $R_w = 0.1014$. There is a large increase in the average Fe−P bond length of 0.27 Å from 149 to 193 K, whereas the Fe−Br bonds only increase by 0.033 Å. The relatively large change in Fe−P bond lengths must be largely responsible for the slow rate of tunneling from the metastable HS state to the stable LS state.

Introduction

In the past decade the kinetics of spin-state interconversions in spin-crossover complexes have received considerable attention.[3] In the solid state, certain Fe^{II} spin-crossover complexes exhibit thermal-, optical-, or pressure-induced switching between the low-spin (LS) and high-spin (HS) states.[4] This may lead to potential applications of these complexes in molecular devices for memory storage or signal processing.[5] In terms of the definition of molecular bistability given by Kahn and Launay,[5] the bistability in spin-crossover systems can be defined as the property of a compound to reversibly interchange between two states, one stable and the other metastable, in response to a controllable external perturbation.

In 1984 Decurtins *et al.*[6] discovered that the spin-crossover complex $[Fe(ptz)_6](BF_4)_2$ (ptz is 1-propyltetrazole) exhibits a light-induced spin-state conversion which was named LIESST (light-induced excited-spin-state trapping). In the LIESST effect, a crystalline sample of this Fe^{II} complex was kept at 10 K and green light was used to convert the whole sample quantitatively from the LS ($^1A_1$) state to the HS ($^5T_2$) state. It was remarkable to find that the whole sample persists for days to weeks in the metastable HS state, providing the crystals are maintained at low temperatures (≤50 K). Hauser later reported[7] the "reverse LIESST" effect, wherein red light is used to convert the metastable HS crystalline sample back to the stable LS form. Thus, crystalline Fe^{II} spin-crossover complexes can be switched between the LS and HS forms at low temperatures using light of different wavelengths. Since this discovery, several other Fe^{II} spin-crossover complexes have been reported[8] to exhibit

⊗ Abstract published in *Advance ACS Abstracts,* October 15, 1997.

(1) University of California at San Diego.
(2) Johannes Gutenberg Universität.
(3) (a) Beattie, J. K. *Adv. Inorg. Chem.* **1988**, *32*, 1. (b) Hauser, A. *Coord. Chem. Rev.* **1991**, *111*, 275. (c) Hauser, A. *Comments Inorg. Chem.* **1995**, *17*, 17.
(4) (a) Gütlich, P. *Struct. Bonding (Berlin)* **1981**, *44*, 83. (b) König, E.; Ritter, G.; Kulshreshta, S. K. *Chem. Rev.* **1985**, *85*, 219. (c) Toftlund, H. *Coord. Chem. Rev.* **1989**, *94*, 67. (d) Goodwin, H. A. *Coord. Chem. Rev.* **1976**, *18*, 293. (e) Gütlich, P. *Adv. Chem. Ser.* **1981**, *194*, 405. (f) Gütlich, P.; Hauser, A.; Spiering, H. *Angew. Chem., Int. Ed. Engl.* **1994**, *33*, 2024. (g) Drickamer, H. G.; Frank, C. W. *Electronic Transitions and the High Pressure Chemistry and Physics of Solids*; Chapman and Hall: London, 1973. (h) Adler, P.; Spiering, H.; Gütlich, P. *Hyperfine Interact.* **1988**, *42*, 1035. (i) Köhler, C. P.; Jakobi, R.; Meissner, E.; Wiehl, L.; Spiering, H.; Gütlich, P. *J. Phys. Chem. Solids* **1990**, *51*, 239. (j) Konno, M.; Mikami-Kido, M. *Bull. Chem. Soc. Jpn.* **1991**, *64*, 339.
(5) Kahn, O.; Launay, J. P. *Chemtronics* **1988**, *3*, 151.
(6) (a) Decurtins, S.; Gütlich, P.; Köhler, C. P.; Spiering, H.; Hauser, A. *Chem. Phys. Lett.* **1984**, *139*, 1. (b) Decurtins, S.; Gütlich, P.; Hasselbach, K. M.; Spiering, H.; Hauser, A. *Inorg. Chem.* **1985**, *24*, 2174.
(7) Hauser, A. *Chem. Phys. Lett.* **1986**, *124*, 543.
(8) (a) Poganiuch, P.; Decurtins, S.; Gütlich, P. *J. Am. Chem. Soc.* **1990**, *112*, 3270. (b) Decurtins, S.; Gütlich, P.; Köhler, C. P.; Spiering, H. *J. Chem. Soc., Chem. Commun.* **1985**, 430. (c) Poganiuch, P.; Gütlich, P. *Inorg. Chem.* **1987**, *26*, 455. (d) Herber, R. *Inorg. Chem.* **1987**, *26*, 173. (e) Poganiuch, P. Masters Thesis, Johannes Gutenberg Universität, 1985. (f) Buchen, Th.; Gütlich, P.; Goodwin, H. A. *Inorg. Chem.* **1994**, *33*, 4573.

S0020-1669(97)00035-9 CCC: $14.00

the LIESST effect, and they are all nitrogen-coordinated Fe^{II} complexes with the ligation of FeN_6.

It is now known that spin-crossover complexes interconvert largely by quantum mechanical tunneling. The first theoretical treatment of tunneling in spin-crossover complexes was given by Buhks *et al*.[9] The first experimental confirmation of tunneling was reported by Xie and Hendrickson.[10] The evidence for tunneling came in the form of a temperature-independent rate for the HS ($^5T_2$) → LS ($^1A_1$) interconversion at temperatures below ~100 K for a specific Fe^{II} complex in a polymer matrix Recently Hauser[3b,c,11] presented detailed laser-flash data for the HS → LS interconversion in order to elucidate the mechanism of the LIESST effect in a series of $Fe^{II}N_6$ complexes. In Hauser's analysis, the extremely longlife time for a complex in the metastable HS state is due to a very slow rate of tunneling from the metastable HS state back to the stable LS state at low temperatures. The differences in metal−ligand bond lengths and energies between complexes in the HS and LS states determine the tunneling rate for the spin-state conversion. Hauser has shown[3b] that there is a correlation of $\ln[k_{HL}(T \rightarrow 0)]$ with $T_{1/2}$, where $k_{HL}(T \rightarrow 0)$ is the extrapolated zero-point tunneling rate and $T_{1/2}$ is the thermal spin transition temperature where there are equal amounts of HS and LS complexes. From this correlation it can be seen that, in order to have the half-life (τ) for low-temperature tunneling longer than 1 h, the $T_{1/2}$ value for an $Fe^{II}N_6$ spin-crossover complex has to be less than ~100 K. A half-life longer than 1 h is necessary in order to monitor the HS → LS relaxation with ^{57}Fe Mössbauer spectroscopy.

In the case of Fe^{II} phosphine compounds, the spin-crossover behavior has been shown to occur for solvated complexes of the general formula *trans*-$[Fe(dppen)_2X_2]\cdot n$S, where dppen is *cis*-1,2-bis(diphenylphosphino)ethylene, X^- is Cl^- or Br^-, and the solvent molecule S is $CHCl_3$, CH_2Cl_2, or $(CH_3)_2CO$.[12] From magnetic susceptibility data for these complexes it has been shown that $T_{1/2}$ is in the temperature range 160−240 K. Also, for some of the complexes, incomplete spin-state conversions have been observed.[12b] Single-crystal X-ray structures have been determined for the acetone solvate of the dichloro complex at 130 and 295 K.[12b] These crystal structures reveal a substantial shortening of the Fe−P bond upon converting from HS to LS, with an average change of ~0.3 Å for all four Fe−P bonds. Very little change (~0.034 Å) was observed in the 130−295 K range for the two Fe−Cl bond lengths. The relatively large change in Fe−P bond lengths between the HS and LS states of these dppen complexes could impact on the rate of quantum mechanical tunneling. Finally, it should be noted that pressure-induced spin-state conversions have also been observed in the two nonsolvated high-spin $[Fe(dppen)_2X_2]$ complexes, where $X^- = Cl^-$ or Br^-, at room temperature.[13]

Even though these dppen Fe^{II} spin-crossover complexes have $T_{1/2} > 165$ K, it was deemed possible that light-induced spin-state conversion to long-lived metastable states may be observed in some of the complexes. An effort was made to observe the LIESST effect at temperatures below 50 K. In this paper, the results of such a study are reported as well as the X-ray structure determination of the chloroform solvate of the dibromo complex and a reinvestigation of the magnetic susceptibility of the four spin-crossover complexes $[Fe(dppen)_2X_2]\cdot 2S$. Relaxation kinetics of the HS → LS conversion occurring after the LIESST effect have also been studied for these four complexes, and the effects of the solvent molecules on this relaxation process are examined.

Experimental Section

Sample Preparation. All reactions and manipulations were carried out in a dry Ar atmosphere. All reagents were obtained from commercial sources and used without further purification. Solvents were used directly from Sure/Seal bottles purchased from the Aldrich Chemical Co.

$[Fe(dppen)_2X_2]\cdot 2S$ [$X^- = Cl^-$, S = $CHCl_3$ (1); $X^- = Cl^-$, S = CH_2Cl_2 (2); $X^- = Br^-$, S = $CHCl_3$ (3); $X^- = Br^-$, S = CH_2Cl_2 (4)]. Samples of these four compounds were synthesized according to the method of Cecconi.[12b] A hot solution of FeX_2 prepared from iron powder and the appropriate acid halide (HX) in absolute ethanol was added to a boiling solution of the ligand in the appropriate solvent (S). Yellow crystals were obtained after slow cooling of the reaction solution. The crystalline products were stored or transported with their mother liquid solution after preparation. The crystalline samples were then filtered off and washed with absolute ethanol directly before any physical measurements. In the literature, the analytical results for complex **1** were reported to indicate that there is *one* solvent molecule (S) per Fe^{II} complex. However, our results indicate that these four complexes (**1**−**4**) are isostructural and all have *two* solvent molecules per iron complex. Anal. Calcd for complex **1**, $C_{52}H_{44}Cl_2FeP_4\cdot C_2H_2Cl_6$: C, 55.99; H, 4.00; Fe, 4.82. Found: C, 56.80; H, 4.11; Fe, 4.65. Calcd for complex **2**, $C_{52}H_{44}Cl_2FeP_4\cdot C_2H_4Cl_4$: C, 59.53; H, 4.44; Fe, 5.13. Found: C, 59.08; H, 4.43; Fe, 5.67. Calcd for complex **3**, $C_{52}H_{44}Br_2FeP_4\cdot C_2H_2Cl_6$: C, 52.00; H, 3.72; Fe, 4.48. Found: C, 52.90; H, 3.82; Fe, 4.44. Calcd for complex **4**, $C_{52}H_{44}Br_2FeP_4\cdot C_2H_2Cl_4$: C, 55.04; H, 4.11; Fe, 4.74. Found: C, 55.47; H, 4.14; Fe, 4.66.

$[Fe(dppen)_2Cl_2]\cdot n CHCl_3$. These partially desolvated samples were obtained either by applying high vacuum ($n = 1.4$) or nitrogen purging ($n = 1.7$) to the crystalline samples of complex **1** for several days. Solvate content *n* was determined by elemental analysis on each sample right before or after each physical measurement. Anal. Calcd for the sample with the $n = 1.4$ solvate, $C_{52}H_{44}Cl_2FeP_4\cdot 1.4CHCl_3$: C, 59.00; H, 4.18. Found: C, 59.02; H, 4.18. Calcd for the sample with the $n = 1.7$ solvate, $C_{52}H_{44}Cl_2FeP_4\cdot 1.7CHCl_3$: C, 57.41; H, 4.10. Found: C, 57.43; H, 4.21.

Magnetic Susceptibility Measurements. The temperature-dependent magnetic susceptibilities of the $[Fe(dppen)_2X_2]\cdot 2S$ compounds were measured using a Quantum Design MPMS SQUID susceptometer. Data were collected in the 30−300 K range at an applied field of 10 kG for each compound. Pascal's constants were used to estimate the diamagnetic correction, which was subtracted from the experimental molar susceptibility values to give the molar paramagnetic susceptibilities of the complexes.

^{57}Fe Mössbauer and Kinetics Measurements. Mössbauer spectra were collected between 8 and 300 K in the transmission geometry. The source was ^{57}Co/Rh kept at room temperature. The samples were sealed in polished Plexiglas containers and mounted in a He-flow cryostat (CF 506, Oxford Instruments), which was equipped with windows of transparent Mylar foil to allow irradiation of the sample with light. LIESST experiments were performed at 10 K using an Ar^+ laser (Coherent, Innova 70) with a 514.5 nm line or a Xe-arc lamp and appropriate filters (reverse LIESST).

Mössbauer spectra were least-squares-fit by employing the transmission integral with the program MOSFUN.[14] In the case of the kinetics measurements, the HS → LS relaxation was followed by monitoring the HS fraction in the temperature interval 28−57 K using Mössbauer spectroscopy. Each spectrum was collected for 30 or 60 min and recorded in sequence.

X-ray Crystallography. X-ray diffraction data were collected for $[Fe(dppen)_2Br_2]\cdot 2CHCl_3$ (**3**) at 149 and 193 K on a Siemens R3m/v

(9) Buhks, E.; Navon, G.; Bixon, M.; Jortner, J. *J. Am. Chem. Soc*. **1980**, *102*, 2918.
(10) Xie, C.-L.; Hendrickson, D. N. *J. Am. Chem. Soc*. **1987**, *109*, 6981.
(11) (a) Hauser, A. *J. Chem. Phys*. **1991**, *94*, 2741. (b) Hauser, A. *Chem. Phys. Lett*. **1990**, *173*, 793.
(12) (a) Levason, W.; McAuliffe, C.; Mahfooz Khan, M.; Nelson, S. M. *J. Chem. Soc., Dalton Trans.* **1975**, 1778. (b) Cecconi, F.; Di Vaira, M.; Midollini, S.; Orlandini, A.; Sacconi, L. *Inorg. Chem*. **1981**, *20*, 3423. (c) König, E.; Ritter, G.; Kulshreshtha, S. K.; Waigel, J.; Sacconi, L. *Inorg. Chem*. **1984**, *23*, 1241.
(13) McCusker, J. K.; Zvagulis, M.; Drickamer, H. H.; Hendrickson, D. N. *Inorg. Chem*. **1989**, *28*, 1380.
(14) Müller, E. W. Ph.D. Thesis, Mainz, 1982. Müller, E. W. *Moessbauer Eff. Ref. Data J*. **1981**, *4*, 89.

Table 1. Summary of Crystal Data and Intensity Collection and Structure Refinement Details for $[Fe(dppen)_2Br_2]\cdot 2CHCl_3$ (**3**)

empirical formula	$C_{54}H_{46}Br_2Cl_6FeP_4$	$C_{54}H_{46}Br_2Cl_6FeP_4$
fw	1247.2	1247.2
crystal system	monoclinic	monoclinic
space group	$P2_1/c$	$P2_1/c$
a, Å	11.636(9)	11.494(16)
b, Å	12.775(13)	12.895(14)
c, Å	18.006(12)	17.49(2)
β, deg	95.48(4)	96.69(10)
V, Å^3	2664(4)	2575(5)
Z	2	2
d(calcd), g/cm^3	1.555	1.609
cryst dimens, mm	0.6 × 0.8 × 1.0	0.6 × 0.8 × 1.0
temp, K	193	149
radiation; λ, Å	Mo Kα; 0.710 73	Mo Kα; 0.710 73
scan speed, deg/min	constant; 10.19	constant; 4.99
scan mode	ω	ω
scan limit, deg	$3 \le 2\theta \le 55.0$	$3 \le 2\theta \le 55.0$
R(int), %	2.49	6.33
no. of unique data	6132	4547
no. of unique data, $F > 4.0\sigma(F)$	4491	3434
no. of variables	264	256
R_F,[a] %	6.02	8.16
R_{wF},[b] %	8.41	10.14
goodness of fit	1.67	1.17

[a] $R_F = \sum(||F_o| - |F_c||)\sum|F_o|$. [b] $R_w = [\sum w(|F_o| - |F_c|)^2/\sum w|F_o|^2]^{1/2}$ where $w = 1/\sigma^2(|F_o|)$.

automated diffractometer using graphite-monochromated Mo Kα radiation ($\lambda = 0.7107$ Å). Lattice constants were determined by least-squares refinement of the angular positions of 14 reflections. The computer program used in the crystallographic calculations was Siemens SHELXTL PLUS (PC version).

To avoid deterioration of crystal quality due to desolvation at room temperature, complex **3** was cooled to 193 K for data collection. The crystal data, intensity collections, and structure refinement are summarized in Table 1. In the full-matrix least-squares refinement, anisotropic temperature factors were used for all non-hydrogen atoms in $[Fe(dppen)_2Br_2]$. The preliminary results of the structure refinement showed very large thermal anisotropic factors for the C and Cl atoms in the solvent $CHCl_3$ molecule. This disperse electron density around the $CHCl_3$ solvent position has been resolved to be three disordered groups with occupancy ratios of 2/1/1 (50%/25%/25%). The three disordered solvent molecules are located in positions wherein the central C atoms are in contact. The two disordered $CHCl_3$ molecules with the lower occupancies (25% and 25%) are very close to each other in position such that their structures can only be refined with isotropic thermal factors for the atomic displacement coefficients. The third solvent molecule with the largest occupancy (50%) is in a position where its three chlorine atoms are staggered with respect to those of the other two disordered solvates. The three C−H bonds of these three $CHCl_3$ molecules are almost coplanar with dihedral angles of ∼15−30° between the C−H bonds. The atomic positional parameters are given in Table 2. Selected bond distances and angles for the central atoms of complex **3** at 193 K are given in Table 3.

The same crystal of complex **3** was used for data collection at 149 K. Some fracturing of the crystal and line broadening of reflection peaks were observed at temperatures right above the spin-state interconversion (∼175 K). The unit cell parameters were obtained by least-squares fitting of the automatically centered setting of 14 reflections. The experimental parameters associated with the data collection can be found in Table 1. This structure was also solved by the heavy-atom method, using heavy-atom positions determined from a sharpened Patterson map. The final positional parameters for all refined atoms and selected bond distances and angles of the central atoms for structures of complex **3** at 149 K are given in Tables 4 and 5, respectively. The chloroform solvent molecules were found to be disordered in two positions at 149 K. After several least-squares-fitting cycles, the final occupancy ratio for the two disordered solvate groups was found to be 90/10 at 149 K.

Table 2. Positional Parameters for $[Fe(dppen)_2Br_2]\cdot 2CHCl_3$ (**3**) at 193 K

atom	*x*/*a*	*y*/*b*	*z*/*c*
Fe	0.5000	0.0000	0.0000
Br(1)	0.3258(1)	0.0712(1)	0.0549(1)
P(1)	0.4818(1)	0.1112(1)	−0.1206(1)
P(2)	0.3754(1)	−0.1168(1)	−0.0923(1)
C(2)	0.6933(3)	0.1455(3)	−0.1832(2)
C(3)	0.7933	0.2013	−0.1918
C(4)	0.8120	0.2958	−0.1556
C(5)	0.7306	0.3344	−0.1109
C(6)	0.6306	0.2786	−0.1024
C(1)	0.6120	0.1841	−0.1385
C(8)	0.2645(3)	0.2053(3)	−0.1203(2)
C(9)	0.1739	0.2678	−0.1482
C(10)	0.1853	0.3283	−0.2107
C(11)	0.2872	0.3263	−0.2453
C(12)	0.3779	0.2638	−0.2174
C(7)	0.3665	0.2033	−0.1549
C(14)	0.1590(3)	−0.1259(3)	−0.0406(2)
C(15)	0.0412	−0.1084	−0.0425
C(16)	−0.0159	−0.0595	−0.1033
C(17)	0.0448	−0.0281	−0.1622
C(18)	0.1626	−0.0457	−0.1604
C(13)	0.2197	−0.0945	−0.0996
C(20)	0.4944(3)	−0.3059(3)	−0.0853(3)
C(21)	0.5056	−0.4133	−0.0876
C(22)	0.4087	−0.4753	−0.1018
C(23)	0.3007	−0.4299	−0.1137
C(24)	0.2896	−0.3225	−0.1115
C(19)	0.3864	−0.2605	−0.0973
C(25)	0.4132(4)	−0.0762(4)	−0.1840(3)
C(26)	0.4606(4)	0.0156(4)	−0.1952(3)
C(1A)	0.8782(4)	−0.3491(4)	−0.1148(3)
Cl(1A)	0.7655	−0.4060	−0.1757
Cl(2A)	0.8456	−0.3511	−0.0201
Cl(3A)	1.0145	−0.4081	−0.1255
C(1B)	0.9020(10)	−0.3473(9)	−0.0758(7)
Cl(1B)	1.0286	−0.3606	−0.0125
Cl(2B)	0.7758	−0.3886	−0.0351
Cl(3B)	0.9166	−0.4123	−0.1620
C(1C)	0.0520(12)	−0.6581(10)	0.0797(7)
Cl(1C)	0.0121	−0.6606	0.1728
Cl(2C)	−0.0012	−0.5441	0.0306
Cl(3C)	0.2039	−0.6728	0.0771

Table 3. Selected Bond Distances and Angles for the Central Atoms of $[Fe(dppen)_2Br_2]\cdot 2CHCl_3$ (**3**) at 193 K

Bond Distances (Å)			
Fe−Br(1)	2.509 (3)	P(1)−C(26)	1.816 (6)
Fe−P(1)	2.586 (3)	P(2)−C(13)	1.827 (4)
Fe−P(2)	2.575 (3)	P(2)−C(19)	1.844 (5)
P(1)−C(1)	1.833 (5)	P(2)−C(25)	1.823 (6)
P(1)−C(7)	1.846 (4)	C(25)−C(26)	1.320 (8)

Bond Angles (deg)			
Br(1)−Fe−P(1)	97.3(1)	Fe−P(2)−C(13)	116.7(1)
Br(1)−Fe−P(2)	92.2(1)	Fe−P(2)−C(19)	124.8(1)
P(1)−Fe−P(2)	77.3(1)	C(13)−P(2)−C(19)	103.0(2)
Fe−P(1)−C(1)	115.1(1)	Fe−P(2)−C(25)	104.5(2)
Fe−P(1)−C(7)	129.0(1)	C(13)−P(2)−C(25)	102.4(2)
C(1)−P(1)−C(7)	101.7(2)	C(19)−P(2)−C(25)	102.4(2)
Fe−P(1)−C(26)	104.2(2)	P(2)−C(25)−C(26)	122.1(4)
C(1)−P(1)−C(26)	105.5(2)	P(1)−C(26)−C(25)	120.9(4)
C(7)−P(1)−C(26)	97.9(2)		

Results and Discussion

Spin-Crossover Behavior. Previously Cecconi *et al.*[12b] reported that samples of *trans*-$[Fe(dppen)_2X_2]\cdot n$S exhibit the spin-crossover phenomenon. In the cases of the two $X^- = Br^-$ complexes, where S is either $CHCl_3$ (complex **3**) or CH_2Cl_2 (complex **4**), they reported that plots of μ_{eff} *vs* temperature showed "residual paramagnetism". That is, when complexes **3** and **4** were cooled to low temperatures, μ_{eff} would not decrease to a low value but would plateau at a value of ∼2.2 μ_B.

Table 4. Positional Parameters for $[Fe(dppen)_2Br_2]\cdot 2CHCl_3$ (**3**) at 149 K

atom	*x*/*a*	*y*/*b*	*z*/*c*
Fe	0.5000	0.0000	0.0000
Br(1)	0.3244(1)	0.0651(1)	0.0544(1)
P(1)	0.4927(2)	0.1089(2)	−0.1065(1)
P(2)	0.3902(2)	−0.1050(2)	−0.0864(1)
C(2)	0.7089(4)	0.1461(3)	−0.1657(3)
C(3)	0.8062	0.2045	−0.1763
C(4)	0.8185	0.3029	−0.1456
C(5)	0.7335	0.3428	−0.1044
C(6)	0.6361	0.2844	−0.0939
C(1)	0.6238	0.1860	−0.1245
C(8)	0.2666(4)	0.2027(5)	−0.1156(3)
C(9)	0.1176	0.2639	−0.1479
C(10)	0.1962	0.3263	−0.2081
C(11)	0.3038	0.3275	−0.2359
C(12)	0.3927	0.2663	−0.2036
C(7)	0.3741	0.2039	−0.1434
C(14)	0.1642(4)	−0.1292(4)	−0.0400(3)
C(15)	0.0457	−0.1149	−0.0431
C(16)	−0.0108	−0.0629	−0.1025
C(17)	0.0512	−0.0251	−0.1588
C(18)	0.1697	−0.0394	−0.1558
C(13)	0.2262	−0.0915	−0.0964
C(20)	0.5138(4)	−0.2923(4)	−0.0663(3)
C(21)	0.5275	−0.3992	−0.0724
C(22)	0.4368	−0.4600	−0.1041
C(23)	0.3325	−0.4139	−0.1299
C(24)	0.3188	−0.3071	−0.1238
C(19)	0.4095	−0.2463	−0.0921
C(25)	0.4206(6)	−0.0654(7)	−0.1827(4)
C(26)	0.4696(7)	0.0242(7)	−0.1903(4)
C(1A)	0.8908(5)	−0.3459(7)	−0.1133(2)
Cl(1A)	0.7763	−0.3992	−0.1749
Cl(2A)	0.8647	−0.3604	−0.0178
Cl(3A)	1.0272	−0.3986	−0.1315
C(1B)	0.0526(36)	−0.6550(35)	0.0599(26)
Cl(1B)	−0.0155	−0.6187	0.1397
Cl(2B)	0.0601	−0.5486	−0.0037
Cl(3B)	0.1917	−0.7111	0.0847

Table 5. Selected Bond Distances and Angles for the Central Atoms of $[Fe(dppen)_2Br_2]\cdot 2CHCl_3$ (**3**) at 149 K

Bond Distance (Å)			
Fe−Br(1)	2.476(4)	P(1)−C(26)	1.822(8)
Fe−P(1)	2.326(4)	P(2)−C(13)	1.881(6)
Fe−P(2)	2.294(4)	P(2)−C(19)	1.840(6)
P(1)−C(1)	1.863(6)	P(2)−C(25)	1.833(8)
P(1)−C(7)	1.890(6)	C(25)−C(26)	1.299(12)
Bond Angles (deg)			
Br(1)−Fe−P(1)	98.5(1)	Fe−P(2)−C(13)	118.3(2)
Br(1)−Fe−P(2)	92.4(1)	Fe−P(2)−C(19)	124.0(2)
P(1)−Fe−P(2)	82.2(1)	C(13)−P(2)−C(19)	102.3(3)
Fe−P(1)−C(1)	120.3(2)	Fe−P(2)−C(25)	107.0(3)
Fe−P(1)−C(7)	128.5(2)	C(13)−P(2)−C(25)	100.7(3)
C(1)−P(1)−C(7)	99.3(2)	C(19)−P(2)−C(25)	100.9(3)
Fe−P(1)−C(26)	105.7(3)	P(2)−C(25)−C(26)	118.2(6)
C(1)−P(1)−C(26)	103.2(3)	P(1)−C(26)−C(25)	118.4(6)
C(7)−P(1)−C(26)	94.7(3)		

Furthermore, it was also reported[12b] that in the case where $X^- = Cl^-$ and S = $CHCl_3$ (complex **1**) there was only one solvent molecule, *i.e.*, $n = 1$, whereas in the other complexes $n = 2$. Since sample quality is important in the spin-crossover and LIESST phenomena, we reinvestigated the nature of these dppen complexes. It was found that all four complexes have two solvent molecules ($n = 2$) per formula and all four complexes are isostructural. It was also found that when the $X^- = Br^-$ complexes are crystalline and have their full complement of solvent molecules, complexes **3** and **4** do not show a residual moment in μ_{eff} at low temperatures.

Plots of μ_{eff} *vs* temperature are shown in Figure 1 for the four dppen complexes. For each complex, the value of μ_{eff} varies from ∼5 μ_B at room temperature to ∼0.5−0.7 μ_B at 10.0 K. The room-temperature value is appropriate for a high-spin Fe^{II} complex with a $^5T_2$ (assuming octahedral symmetry) ground state. At low temperatures, all four complexes are low-spin Fe^{II} complexes with a $^1A_1$ ground state. The ∼0.5−0.7 μ_B value of μ_{eff} is attributable to temperature-independent paramagnetism.

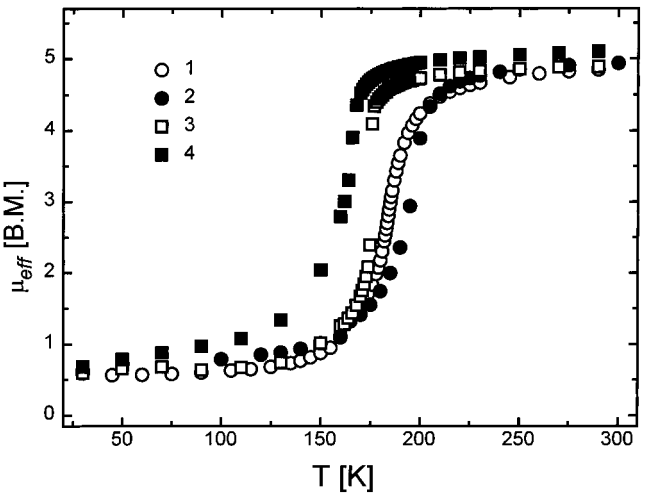

Figure 1. Temperature dependence of the effective magnetic moment, μ_{eff}: ○, $[Fe(dppen)_2Cl_2]\cdot 2CHCl_3$ (**1**); ●, $[Fe(dppen)_2Cl_2]\cdot 2CH_2Cl_2$ (**2**); □, $[Fe(dppen)_2Br_2]\cdot 2CHCl_3$ (**3**); ■, $[Fe(dppen)_2Br_2]\cdot 2CH_2Cl_2$ (**4**).

The temperature at which there are equal amounts of HS and LS complexes, $T_{1/2}$, was evaluated from the plot of μ_{eff} *vs* temperature for each complex. The $T_{1/2}$ values for the two dichloro complexes **1** ($T_{1/2}$ = 185 K) and **2** ($T_{1/2}$ = 195 K) are higher than those for the dibromo complexes **3** ($T_{1/2}$ = 175 K) and **4** (T = 165 K). A detailed analysis (first derivatives) of the μ_{eff} *vs* temperature plots shows that the spin-crossover transformation is more abrupt for the two dibromo complexes than for the two dichloro complexes. This relatively more abrupt conversion for the dibromo complexes suggests that there is greater cooperativity for the conversion in the dibromo complexes. The higher $T_{1/2}$ values for the two dichloro complexes could reflect the fact that the Cl^- ligand has a greater ligand-field strength than does the Br^- ligand. This leads to a greater crystal-field splitting for the dichloro complexes and, consequently, a larger energy difference between low-spin $^1A_1$ and high-spin $^5T_2$ states. For complexes with different solvent molecules there is no simple correlation between $T_{1/2}$ and which solvent molecule, $CHCl_3$ or CH_2Cl_2, is present. For the dichloro complexes, the $T_{1/2}$ of the $CHCl_3$ solvate (**1**) is lower than that of the CH_2Cl_2 solvate (**2**), whereas for the dibromo complexes the reverse order in $T_{1/2}$ holds for complexes **3** and **4**.

X-ray Crystal Structure of Complex 3. Cecconi *et al.*[12b] reported the X-ray structure of $[Fe(dppen)_2Cl_2]\cdot 2(CH_3)_2CO$ at 295 and 130 K. At 295 K, the space group was found to be $P2_1/a$. A few data of poor quality were obtained on crystals at 130 K. The diffraction pattern of the material at 130 K was not rigorously consistent with either the symmetry requirements of the Laue group $P2/m$ or the systematic absences of the space group $P2_1/a$. Nevertheless, the refinement of the structure at 130 K was carried out in the space group $P2_1/a$ found at 295 K. The 130 K data indicated that the acetone solvent molecules are distributed almost equally between two different orientations. At 295 K, the acetone molecule was refined as a rigid group with idealized geometry.

In view of the uncertainties in the X-ray crystallography[12b] of the dichloro−acetone complex, we determined the X-ray structure of $[Fe(dppen)_2Br_2]\cdot 2CHCl_3$ (complex **3**) at 149 and 193 K. The temperature of 193 K was selected because this is

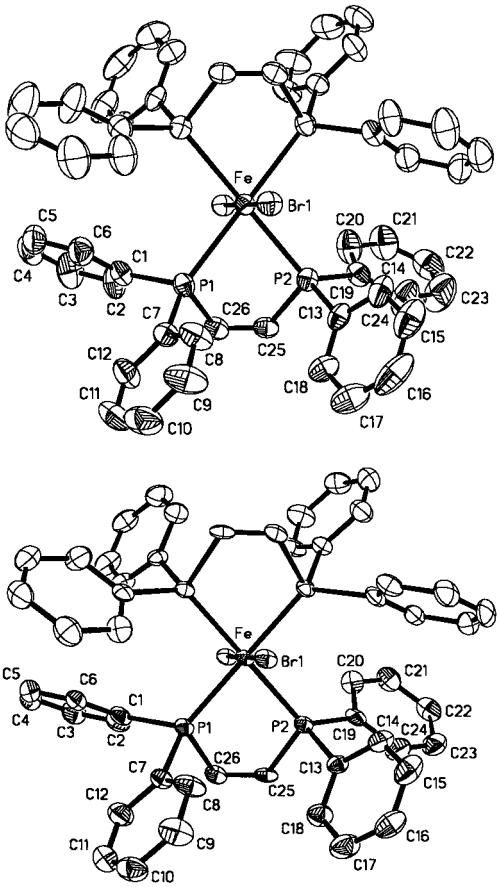

Figure 2. ORTEP plot of the molecular structure of $[Fe(dppen)_2Br_2]$ in the $CHCl_3$ solvate **3** at 193 K (top) and at 149 K (bottom). Atoms are shown as 40% equiprobability ellipsoids.

just above the conversion to HS. At 149 K, complex **3** is completely LS. It was found (see Table 1) that complex **3** adopts the monoclinic space group $P2_1/c$ with $Z = 2$ at both 149 and 193 K. In Figure 2 are shown the perspective views of the $[Fe(dppen)_2Br_2]$ molecule at 149 and 193 K. From the results of the structural refinement, it is found that complex **3** is isostructural with $[Fe(dppen)_2Cl_2]\cdot 2(CH_3)_2CO$ at 295 K.

The overall molecular conformations of $[Fe(dppen)_2Br_2]$ in complex **3** at 149 and 193 K and the dichloro−acetone complex at 295 K are very similar. Thus, neither a change in the X^- ligand nor a change from HS to LS affects the conformation of the $[Fe(dppen)_2X_2]$ molecule. The iron−dppen complex has crystallographic C_i symmetry. The iron atom lies strictly in the plane of the four phosphorus atoms. The Fe−X bond is tipped at an angle of ∼10° to the normal of the FeP_4 plane. In the molecules shown in Figure 2, the atoms drawn as open ellipsoids were generated by the symmetry operation of inversion.

Comparison of the bond distances and angles given in Tables 3 and 5 for complex **3** at 193 and 149 K, respectively, shows there are appreciable changes in the dimensions of the $[Fe(dppen)_2Br_2]$ molecule in converting from HS to LS. The largest bond length change occurs in the Fe−P bonds where the average Fe−P bond length decreases by 0.27 Å in going from 193 to 149 K. The corresponding decrease in the Fe−Br bond length of 0.033 Å is an order of magnitude smaller. The 0.27 Å decrease in average Fe−P bond length is larger than any decrease reported[4] for $Fe^{II}N_6$ type spin-crossover complexes, where changes as large as 0.20 Å in average Fe−N bond lengths are seen. The variations in bond angles in $[Fe(dppen)_2Br_2]$ between 193 and 149 K are all relatively small (<1°). Thus, the main structural change occurring in the HS to LS conversion in complex **3** occurs in the Fe−P bond lengths.

Figure 3 shows a stereoscopic view of the packing arrangement in $[Fe(dppen)_2Br_2]\cdot 2CHCl_3$ (**3**) at 149 K. There are two iron complexes and four solvent molecules in the monoclinic unit cell. The Fe−dppen complex located at the center of Figure 3 is surrounded by six other Fe−dppen complexes and four $CHCl_3$ solvent molecules. For this central Fe−dppen complex it can be seen that, above and below the FeP_4 plane, there is a $CHCl_3$ solvent molecule located in the "pocket" made of phenyl groups. The average contact distance between the hydrogen atom of the $CHCl_3$ solvent molecule and the Br^- ligand is ∼4.05 Å for complex **3** when it is in the HS state (193 K). In spite of the more compact crystal lattice at 149 K, these $H\cdots Br^-$ contact distances are actually larger by ∼0.1 Å. In the case of the dichloro complexes, X-ray structures[15] show that the $H\cdots Cl^-$ contact distances with the solvent molecule are ∼4.45 Å for the HS and ∼4.55 Å for the LS form of the crystal. Thus, the Br^- ion is closer to the $CHCl_3$ solvent molecule than is the Cl^- ion in the $[Fe(dppen)_2X_2]$ solvates. This could explain the somewhat greater cooperativity, *i.e.*, more abruptness, in the HS to LS conversion for the two dibromo complexes. The longer solvate···X^- distances in the LS crystals likely reflect the fact that the Fe−P bonds are shorter, which pulls in the phenyl groups and closes the pocket above the halide ion.

In Figure 4 are given stereoscopic views of the disordered solvent chloroform molecules in $[Fe(dppen)_2Br_2]\cdot 2CHCl_3$ (**3**) at 193 and 149 K. The disordered structures of chloroform molecules in Figure 4 were determined for the same single crystal. At 193 K, where complex **3** is in the HS state, the chloroform solvate is severely disordered in three positions. The occupancy ratios for these three disordered groups at 193 K are 50/25/25 (C(1A)/C(1B)/C(1C)). The disordered group C(1A) with 50% occupancy is plotted with solid bonds and ellipsoids in Figure 4A. The angles between the C−H bonds of these three disordered $CHCl_3$ molecules are ∼30−45°. As the temperature of the crystal is lowered to 149 K, where complex **3** converts to the LS form, the chloroform solvate becomes disordered in only two positions (Figure 4B). The refined occupancy ratio for these two disordered groups at 149 K is 90/10 (C(1A)/C(1B)). The disorder structure of solvate molecules at 149 K in complex **3** has retained two disorder elements from the structure at 193 K. However, the relatively large occupancy (90%) for one disorder element (C(1A)) in the solvate structure at 149 K indicates that the disordered structure of the solvate molecules has almost disappeared as complex **3** converts from the HS state at high temperatures to the LS state at low temperatures. The disappearance of disorder strongly suggests that the solvate molecule has undergone an order−disorder transition, possibly involving a transformation from a dynamically disordered structure at high temperatures to a statically disordered structure at low temperatures.[16] The HS to LS conversion of complex **3** could be influenced by the order−disorder transformation of the solvent molecule.

LIESST Effect and HS → LS Relaxation Kinetics. Crystalline samples of the four $Fe^{II}X_2P_4$ complexes were examined with ^{57}Fe Mössbauer spectroscopy. All four complexes convert from the HS form at high temperatures with one Mössbauer doublet characteristic of a HS Fe^{II} complex to the LS form at low temperatures with a single doublet characteristic of a LS Fe^{II} complex. All four complexes exhibit the LIESST effect as demonstrated in Figure 5.

(15) Wu, C.-C.; Gantzel, P. D.; Hendrickson, D. N. Unpublished results.
(16) Rao, C. N.; Rao, K. J. *Phase Transition in Solids*; McGraw-Hill: New York, 1978.

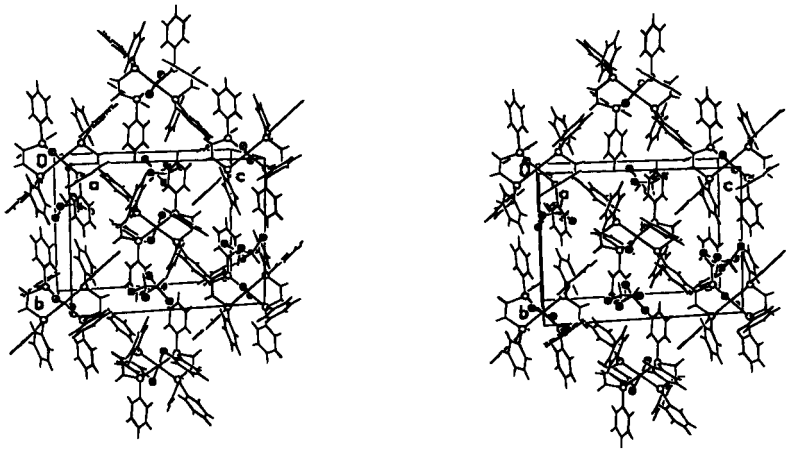

Figure 3. Stereoscopic view of the packing arrangement in the monoclinic $P2_1/c$ crystal of $[Fe(dppen)_2Br_2]\cdot 2CHCl_3$ at 149 K. In the unit cell, each of the Fe^{II} complexes is associated with two $CHCl_3$ solvate molecules and each of these is disordered in two positions.

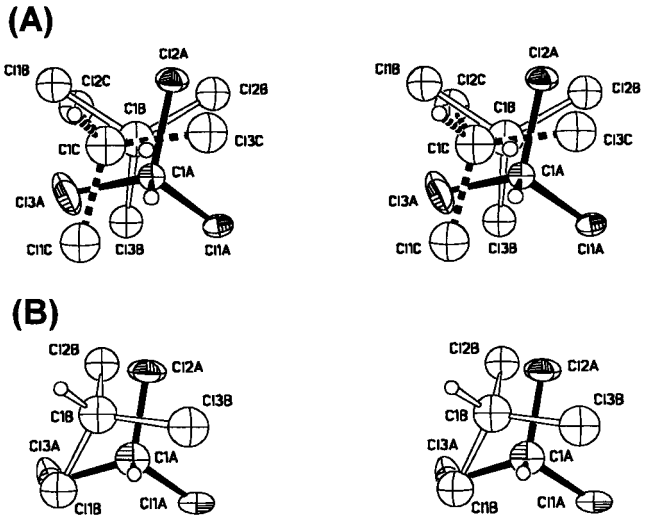

Figure 4. Stereoscopic views of the disordered $CHCl_3$ solvate molecule in $[Fe(dppen)_2Br_2]\cdot 2CHCl_3$ (**3**) at 193 K (A) and 149 K (B). Atoms are shown as 10% equiprobability ellipsoids in (A) and 20% equiprobability ellipsoids in (B).

A HS doublet (trace A) with a quadrupole splitting of $\Delta E_Q = 2.507(11)$ mm/s and an isomer shift of $\delta = 0.696(10)$ mm/s (*vs* iron foil) is observed at 295 K for complex **1**. When the sample is cooled to 10.2(2) K, a LS doublet with $\Delta E_Q = 0.679(7)$ mm/s and an isomer shift of $\delta = 0.384(6)$ mm/s is detected (trace B). As can be seen in trace C, irradiation of the sample maintained at 12 K with an Ar ion laser (514.5 nm line) for 90 min converts the LS sample almost totally to a HS sample. This metastable HS form persists for several hours at 12 K. Trace D shows that the reverse LIESST effect is also possible. After LIESST, the sample is maintained at 12 K and irradiated for 3 h with a xenon high-pressure lamp filtered so that $\lambda > 695$ nm (red) converts some of the metastable HS complexes back to the stable LS form. Complete back-conversion is probably not observed because a dynamic equilibrium is achieved due to the broad-band irradiation, as seen before.[11a]

The relaxation kinetics of HS to LS state transitions for the four dppen complexes were studied following the LIESST effect at 10 K. Figure 6 shows the relaxation of a sample of $[Fe(dppen)_2Cl_2]\cdot 2CHCl_3$ (**1**) at six temperatures below 40 K. For each run, the crystalline sample was cooled to 10 K, irradiated for 90 min with a Ar ion laser until full spin conversion was achieved, and then in a few minutes warmed to some higher temperature (27.9, 31.5, 33.9, 35.9, 37.4, or 39.6 K). At the higher temperatures Mössbauer spectra were collected every 30

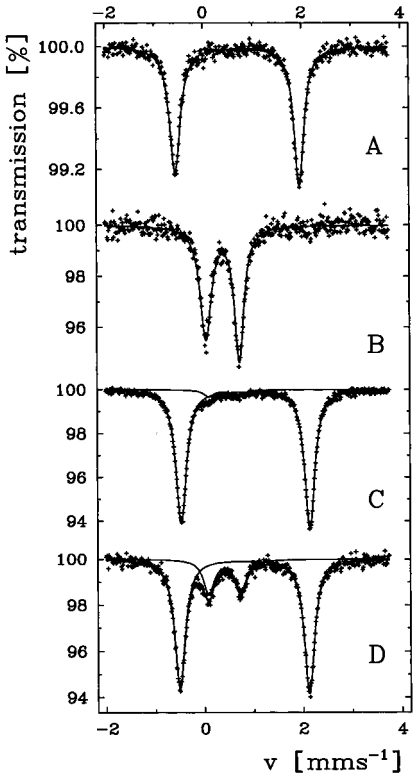

Figure 5. ^{57}Fe Mössbauer spectra for a polycrystalline sample of $[Fe(dppen)_2Cl_2]\cdot 2CHCl_3$ (**1**). A HS doublet is observed at 295 K (A), whereas cooling the sample to 10.2(2) K gives a LS doublet (B). Trace C was run at 10 K after the sample was irradiated for 90 min with an Ar ion laser while being maintained at 12 K (LIESST effect). In trace D, the reverse LIESST effect is shown where, after LIESST, the sample was maintained at 12 K and irradiated for 3 h with red light (filtered Xe lamp; $\lambda > 695$ nm) to convert ~15% of the metastable HS complexes back to the stable LS state.

or 60 min to monitor the reappearance of the stable LS form, which occurs at the expense of complexes in the metastable HS form. The two doublets in each spectrum were fit to give the ratio of t_{HS}/t_{total} (spectral "thickness" of HS signal compared to total "thickness", i.e., the ratio of spectral areas). This ratio is taken to be equal to the fraction (γ_{HS}) of HS complexes, which is plotted in Figure 6 *vs* time for the above six different temperatures. It can be seen that, at the lowest temperature (27.9 K), 90% of the metastable HS complexes relax back to the LS state in ~4.6 days. HS → LS relaxation data were also collected for complexes **2**−**4** by following the above experimental procedure in different temperature ranges. In Figure 7

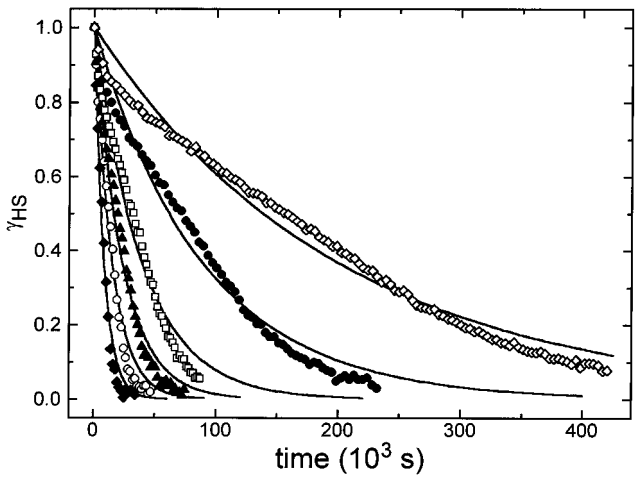

Figure 6. HS → LS relaxation curves after LIESST of [Fe(dppen)$_2$Cl$_2$]·2CHCl$_3$ (**1**) at six different temperatures: ◇, 27.9 K; ●, 31.5 K; □, 33.9 K; ▲, 35.9 K; ○, 37.4 K; ◆, 39.6 K. Each data point represents the HS fraction derived from a single Mössbauer spectrum. The solid lines are the results of least-squares fits to single-exponential relaxation curves.

are given the relaxation curves for complex 2. The data for complexes **3** and **4** are available in the Supporting Information.

Three interesting observations have been made on the relaxation kinetics after LIESST in the four dppen complexes. First, the relaxation kinetics are complicated for these complexes. Second, there is a solvent molecule dependence of the relaxation rates for the four [Fe(dppen)$_2$X$_2$]·2S complexes. Finally, and most importantly, these dppen complexes show relatively slow rates for the metastable HS to stable LS state relaxation even though the $T_{1/2}$ temperatures for the thermal spin-state conversions are in the range 164−195 K.

If the relaxation of a molecule from the metastable HS state to the LS state after LIESST was a single-molecule response, first-order kinetics would be seen. The rate of appearance of LS complexes would be given by

$$d\gamma_{LS}/dt = k_{HL}(1 - \gamma_{LS}) \qquad (1)$$

In this equation k_{HL} is the rate constant for the HS → LS conversion. As can be seen in Figure 6, the relaxation data for complex **1** can be reasonably well fit by single-exponential relaxation curves. In Table 6 are summarized the fitting parameters obtained by least-squares-fitting the relaxation data for complex **1** to single exponentials.

It is interesting that the relaxation data obtained for complexes **2**−**4** do not fit well to single-exponential relaxation curves. This can be seen by comparing the data shown in Figure 7 for complex **2** with those shown in Figure 6 for complex **1**. The relaxation curves for complexes **2**−**4** are sigmoidal, suggesting that for these complexes the HS → LS relaxation is not just for an isolated molecule. There must be some cooperativity present. Previous studies of HS → LS relaxation in Fe^{II}N$_6$ spin-crossover complexes have shown similar results. In general, it has been found that when an Fe^{II}N$_6$ complex is doped into a solid, *e.g.*, [Zn$_{1-x}$Fe$_x$(ptz)$_6$](BF$_4$)$_2$], a single-exponential type of HS → LS relaxation is observed.[4f] When a nondoped solid such as [Fe(ptz)$_6$](BF$_4$)$_2$ is studied, sigmoidal relaxation curves may be seen. The sigmoidal relaxation curves can be interpreted as a self-acceleration of the HS → LS relaxation with increasing proportions of LS complexes, *i.e.*, increasing γ_{LS}. It has been shown[17,18] that phenomenologically the acceleration results from the buildup of an internal pressure ("lattice pressure") with increasing LS proportions. This "lattice pressure" is caused by the large reduction in size of a Fe^{II} spin-crossover complex as it converts from HS to LS. Hauser *et al.*[17,18] showed that the relaxation rate is a function of this "lattice pressure" and therefore is also a function of the LS proportion γ_{LS}. Equation 1 still is appropriate, but now k_{HL} is no longer a constant but is a function of γ_{LS} as in

$$k_{HL}(\gamma_{LS}, T) = k^\circ_{HL}(T)\, e^{a(T)\gamma_{LS}} \qquad (2)$$

In eq 2 $k^\circ_{HL}(T)$ is the relaxation rate constant for the complex in a cooperative environment, *i.e.*, in a sufficiently concentrated mixed crystal with high iron concentration. In concentrated spin-crossover crystals, cooperative interactions become more and more important. Spiering *et al.*[19,20] have shown that such cooperative interactions can be described as being elastic in nature; a model based on concepts of elasticity theory has been employed successfully to reproduce the phenomenological interaction constants.

The solid lines shown in Figure 7 result from a least-squares fit of the relaxation data for complex **2** to eqs 1 and 2. It can be seen that quite reasonable fits of the data have been found where the rate constant k_{HL} depends on γ_{LS}. The fitting parameters are summarized in Table 6. Thus, the data for complex **1** are fit reasonably well by single-exponential relaxation curves, but the relaxation data for complexes **2**−**4** require a γ_{LS}-dependent rate constant. In the case of complexes **2**−**4**, least-squares fits of the relaxation data were obtained by assuming that the coefficient $a(T)$ is a constant at each different temperature. If the HS → LS relaxation follows the cooperative model of eq 2, then a plot of ln(k_{HL}) *vs* γ_{HS} should give a straight line with nonzero slope. This, however, has not been observed for any of the four dppen complexes.

Table 6. Least-Squares-Fitting Parameters for the HS → LS Relaxation Kinetics of [Fe(dppen)$_2$X$_2$]·2S

I. First-Order Kinetics: $\gamma_{HS} = a_0 \exp[-k_{HL}(T)t]$

[Fe(dppen)$_2$Cl$_2$]·2CHCl$_3$ (**1**)

T, K	a_0	k_{HL} (T), s^{-1}	T, K	a_0	k_{HL} (T), s^{-1}
27.9	1	5.0(1) × 10^{-6}	35.9	1	4.27(10) × 10^{-5}
31.5	1	1.13(2) × 10^{-5}	37.4	1	6.69(24) × 10^{-5}
33.9	1	2.54(1) × 10^{-5}	39.6	1	1.192(48) × 10^{-4}

II. γ_{HS}-Dependent Kinetics: $k_{HL}(\gamma_{HS}, T) = k^\circ_{HL}(T) \exp[a(T)(1 - \gamma_{HS})]$, $0.1 \le \gamma_{HS} \le 1.0$

[Fe(dppen)$_2$Cl$_2$]·2CH$_2$Cl$_2$ (**2**)

T, K	$a(T)$	$k^\circ_{HL}(T)$, s^{-1}	T, K	$a(T)$	$k^\circ_{HL}(T)$, s^{-1}
40.9	4.32(13)	1.09(11) × 10^{-4}	46.0	4.04(30)	6.87(168) × 10^{-4}
42.0	3.79(18)	1.17(18) × 10^{-4}	47.9	4.37(40)	1.65(54) × 10^{-3}
43.9	3.63(28)	2.20(50) × 10^{-4}			

[Fe(dppen)$_2$Br$_2$]·2CHCl$_3$ (**3**)

T, K	$a(T)$	$k^\circ_{HL}(T)$, s^{-1}	T, K	$a(T)$	$k^\circ_{HL}(T)$, s^{-1}
54.0	3.69(13)	1.96(2) × 10^{-4}	56.0	4.21(28)	6.42(150) × 10^{-4}
55.0	4.63(28)	6.08(134) × 10^{-4}	57.0	5.02(51)	1.67(68) × 10^{-3}

[Fe(dppen)$_2$Br$_2$]·2CH$_2$Cl$_2$ (**4**)

T, K	$a(T)$	$k^\circ_{HL}(T)$, s^{-1}	T, K	$a(T)$	$k^\circ_{HL}(T)$, s^{-1}
50.0	3.52(23)	1.42(27) × 10^{-4}	51.9	3.71(27)	3.04(67) × 10^{-4}
51.0	3.64(23)	2.04(38) × 10^{-4}	52.9	4.03(47)	5.4(21) × 10^{-4}

(17) Hauser, A. *Chem. Phys. Lett.* **1992**, *192*, 65.
(18) Hinek, R.; Gütlich, P.; Hauser, A. *Inorg. Chem.* **1994**, *33*, 567.
(19) Spiering, H.; Meissner, E.; Köppen, H.; Müller, E. W.; Gütlich, P. *Chem. Phys.* **1982**, *68*, 65.
(20) Spiering, H.; Willenbacher, N. *J. Phys.: Condens. Matter* **1989**, *1*, 10089.

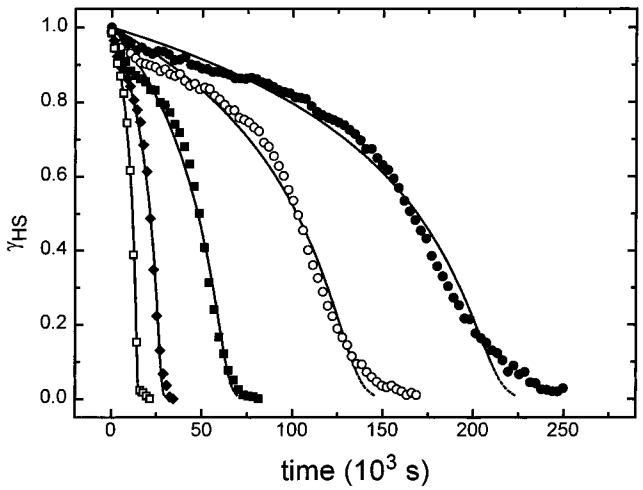

Figure 7. HS → LS relaxation curves after LIESST of [Fe(dppen)$_2$Cl$_2$]·2CH$_2$Cl$_2$ (**2**) at five different temperatures: □, 41.0 K; ◆, 42.0 K; ■, 43.9 K; ○, 46.0 K; ●, 48.0 K. The solid lines are the results of least-squares fits of the data to the HS fraction dependent relaxation kinetics model in the range $\gamma_{HS} = 1-0.1$.

Hauser *et al.*[21] was able to reproduce the HS → LS relaxation curves for the high-temperature phase of [Fe(ptz)$_6$](BF$_4$)$_2$; in this case, the plots of ln[$k_{HL}(\gamma_{HS})$] *vs* γ_{HS} give straight lines. On the other hand, pronounced deviation from linearity for the ln[$k_{HL}(\gamma_{HS})$] *vs* γ_{HS} plots was reported[22] for [Fe(bpp)$_2$](BF$_4$)$_2$, where bpp is 2,6-bis(pyrazol-3-yl)pyridine. The thermal spin transition in [Fe(bpp)$_2$](BF$_4$)$_2$ is accompanied by a structural phase transition. It was suggested[22] that the nonlinear ln(k_{HL}) *vs* γ_{HS} plots resulted from HS → LS tunneling rates which are different in the two crystal phases; the relatively slow rates for the phase transition superimposes on the two tunneling rates.

In the case of the dppen complexes **1**−**4**, no structural phase transition has been observed. However, the dppen complexes do seem to be involved in an order−disorder phase transition involving the solvent molecules in the crystal. From the X-ray structures of [Fe(dppen)$_2$Br$_2$]·CHCl$_3$ (complex **3**) at 149 and 193 K, it is clear that the nature of the disorder in the CHCl$_3$ solvent molecules changes in the thermally driven spin crossover. It appears that the solvent molecules are static at low temperatures and become dynamic at temperatures above the thermal spin crossover. Preliminary solid-state ^{2}H NMR data collected for polycrystalline samples of [Fe(dppen)$_2$Cl$_2$]·2CDCl$_3$ (**1**) and [Fe(dppen)$_2$Br$_2$]·CDCl$_2$ (**3**) indicate that the solvent molecules are increasing their motion in the crystals as the temperature is increased. Furthermore, the natures of the solvent molecule dynamics in these two solids are different.

Low-Temperature Tunneling Rate. The rate constant for HS → LS tunneling at temperatures approaching $T = 0$ K, *i.e.*, $k_{HL}(T \rightarrow 0)$, is an important diagnostic of Fe^{II} spin-crossover complexes. At the lowest temperatures, all of the metastable HS complexes are in their lowest energy vibrational level and the tunneling rate reflects the potential energy barrier. Recently[3b] it was shown that there is a correlation of ln[$k_{HL}(T \rightarrow 0$] with $T_{1/2}$, the temperature of the thermally driven spin crossover. This correlation was established for a series of Fe^{II}N$_6$ spin-crossover complexes. It was desirable to determine $k_{HL}(T \rightarrow 0)$ values for the four Fe^{II}P$_4$X$_2$ dppen complexes. The different types of ligands in the dppen complexes, in particular those with relatively large changes in Fe−P bond lengths, could lead to $k_{HL}(T \rightarrow 0)$ values that do not fit the correlation for Fe^{II}N$_6$ complexes. One goal for complexes exhibiting the LIESST effect is to identify complexes that exhibit slow rates of HL → LS tunneling at higher temperatures.

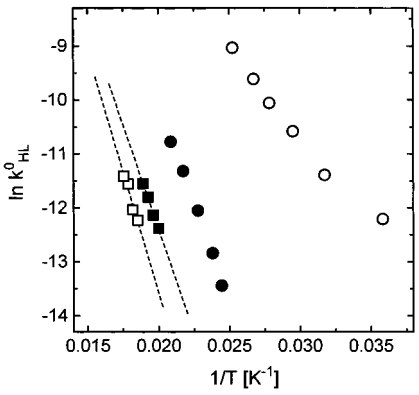

Figure 8. Rate constants for the HS → LS relaxation plotted as ln(k_{HL}) *vs* 1/*T* (Arrhenius plot) for the four Fe^{II}P$_4$X$_2$ complexes: ○, **1**; ●, **2**; □, **3**; ■, **4**.

In Figure 8 is given an Arrhenius type plot of ln($k°_{HL}$) *vs* 1/*T* for the data for complex **1** in the 27.9−39.6 K range. From these data it is clear that there is an activated process at the higher temperatures, but the rate is slowing down at the lowest temperature of 27.9 K. As an *upper* limit, we can take the value of ln(k_{HL}) at 27.9 K, *i.e.*., ln(k_{HL}) = −12.21, as ln[$k_{HL}(T \rightarrow 0)$].

The relaxation data in the range $\gamma_{HS} = 1$ to $\gamma_{HS} = 0.1$ for complexes **2**−**4** were fit with the model for the cooperative self-accelerating relaxation. For Fe^{II}N$_6$ spin-crossover complexes the value of $k°_{HL}(T)$ in non-doped crystalline samples has been found to be equal to the relaxation rate $k_{HL}(T)$ for an isolated molecule found in diluted mixed crystals. In the case of the dppen complexes **2**−**4**, the $k°_{HL}(T)$ values obtained from the least-squares fitting are expected to be close to the temperature-dependent rate constant $k_{HL}(T)$. An Arrhenius plot of the data for complex **2** (X$^-$ = Cl$^-$ and S = CH$_2$Cl$_2$) is shown (●) in Figure 8. The data for **2** were measured at 41.0, 42.0, 43.9, 46.0, and 48.0 K. As an upper limit for ln[$k_{HL}(T \rightarrow 0$), we can take −13.78, the value at the lowest temperature of 41.0 K.

The two dibromo (X$^-$ = Br$^-$) complexes **3** and **4** exhibit the LIESST effect such that a temperature of ∼50−60 K is needed to monitor the relaxation rates with the ^{57}Fe Mössbauer technique. This gave a more limited set of data points for **3** and **4**; see Figure 8. A straight line was fit through the four data points on the Arrhenius plot for complex **3**. This straight line was extrapolated to a 1/*T* value corresponding to $T = 40$ K to estimate a value of ln[$k_{HL}(T \rightarrow 0)$] = −18.09 for complex **3**. A similar extrapolation for complex **4** gave ln[$k_{HL}(T \rightarrow 0)$] = −16.27. The temperature of 40 K was selected as the temperature below which all Fe^{II} spin-crossover complexes have reached their temperature-independent HL → LS tunneling rate.

In Figure 9 is reproduced the correlation of ln[$k_{HL}(T \rightarrow 0)$] with $T_{1/2}$ as determined[3b,4f] for Fe^{II}N$_6$ spin-crossover complexes. The data points for the four Fe^{II}P$_4$X$_2$ dppen complexes have been added to the correlation. It is clear that the points for the four dppen complexes do not fit the correlation for the Fe^{II}N$_6$ complexes. As per previous discussions,[3b] the tunneling rate constant for the HS → LS transition at low temperatures is given by

$$k_{HL}(T \rightarrow 0) = \frac{2\pi}{\hbar\omega}(\beta_{HL})^2(g_f)\left(\frac{S^p e^{-S}}{p!}\right) \qquad (3)$$

In this expression, $\hbar\omega$ is the vibrational frequency for the totally symmetric "breathing mode" of the Fe−ligand atom stretching, β_{HL} is the electronic tunneling matrix element, g_f is the electronic degeneracy of the final state (LS state, $g_f = 1$), p is the reduced

(21) Hauser, A.; Gütlich, P.; Spiering, H. *Inorg. Chem.* **1986**, *25*, 6245.
(22) Buchen, T.; Gütlich, P.; Goodwin, H. A. *Inorg. Chem.* **1994**, *33*, 4573.

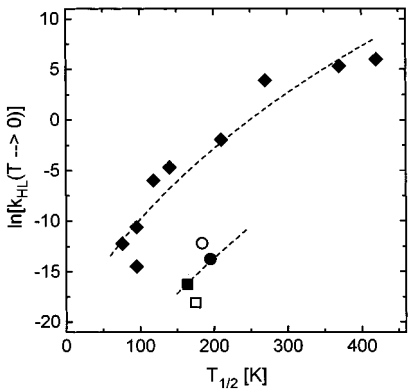

Figure 9. Plots of the low-temperature tunneling rate constant $\ln[k_{HL}(T \rightarrow 0)]$ *vs* the thermal transition temperatures $T_{1/2}$ for the $Fe^{II}N_6$ (◆) spin-crossover complexes (from ref 3b) and for the $Fe^{II}P_4X_2$ complexes (○, **1**; ●, **2**; □, **3**; ■, **4**). The dashed lines are the calculated results for the $Fe^{II}N_6$ complexes with $S \approx 50$ and for the $Fe^{II}P_4X_2$ complexes with $S \approx 60$ (see text).

energy gap defined as the energy difference between the HS and LS states ($\Delta E°_{HL}$) divided by $\hbar\omega$, and S is the Huang−Rhys factor, a measure for the relative horizontal displacement (ΔQ_{HL}) between the HS- and LS-state potential energy wells.

For $Fe^{II}N_6$ complexes β_{HL} has been estimated[3c,9] to be ∼150 cm^{-1} and the average value for $\hbar\omega$ is ∼250 cm^{-1}. With the assumption of a linear relationship between $\Delta E°_{HL}$ and the thermal transition temperature $T_{1/2}$, a fit of the $\ln[k_{HL}(T \rightarrow 0)]$ *vs* $T_{1/2}$ data for $Fe^{II}N_6$ complexes in Figure 9 has given $S \simeq 50$. The theoretical fit line is shown as a dashed line in Figure 9. With the limited data available for four $Fe^{II}P_4X_2$ complexes a value of $S \simeq 60$ fits the data available; see Figure 9. Thus, for a given $T_{1/2}$ value, the $Fe^{II}P_4X_2$ complexes exhibit a much slower rate of low-temperature tunneling than do the $Fe^{II}N_6$ complexes, because the Huang−Rhys factor for the $Fe^{II}P_4X_2$ complexes is larger. This is probably a reflection of the larger bond length changes observed for the $Fe^{II}P_4X_2$ complexes compared to the $Fe^{II}N_6$ complexes. In the LS → HS conversion of $Fe^{II}N_6$ spin-crossover complexes, the Fe−N bond length increases by 0.16−0.21 Å.[3,4] The corresponding Huang−Rhys factor is predicted to be S ∼ 40−50. The results of the 149 and 193 K X-ray structure determinations for $[Fe(dppen)_2Br_2]\cdot 2CHCl_3$ (complex **3**) show that on the average the Fe−P bonds change by 0.27 Å in the LS → HS conversion and the Fe−Br bond length change is only 0.033 Å. The relatively large change in Fe−P bond length is the origin of the larger Huang−Rhys factor. The $Fe^{II}P_4X_2$ complexes have longer lifetimes for the metastable HS state for a given $T_{1/2}$ value. The $Fe^{II}P_4X_2$ complexes exhibit slower rates of low-temperature tunneling because there is a greater horizontal displacement ΔQ_{HL} between the HS- and LS-state potential energy wells than in the $Fe^{II}N_6$ complexes.

It should be pointed out that in Figure 9 only the $Fe^{II}N_6$ complexes with $T_{1/2} \leq 100$ K can be probed with ^{57}Fe Mössbauer spectroscopy; for most of the complexes, the value of k_{HL} is too large to permit the determination of the relaxation kinetics. Laser-flash photolysis was used to obtain the relaxation rates for $Fe^{II}N_6$ complexes with $T_{1/2} > 100$ K. LIESST experiments were carried out in this study also on a sample of $[Fe(dppen)_2Cl_2]\cdot 2CH_3COCH_3$. This acetone solvate has $T_{1/2} = 230$ K.[12] We have found that the HS → LS relaxation is too fast in this complex to monitor the relaxation with ^{57}Fe Mössbauer spectroscopy. In just minutes after laser-light excitation of a sample of this complex at 10 K, the complex had relaxed back to the LS state. This observation is consistent with the correlation shown in Figure 9.

Effects of the Solvent Molecules on Relaxation. For the series of $Fe^{II}P_4X_2$ complexes it has been found in previous studies[12c] that the solvent molecules in the crystal lattice can affect the thermal spin-state conversion in the solid state. Nonsolvated crystalline samples of the $Fe^{II}P_4X_2$ complexes are found to have lattice structures and spin-crossover properties that are totally different from that of solvated ones.[12b] However, it is not clear whether it is the lattice packing, the nature of the solvate molecules, or both that dominate the spin-crossover properties for the dppen complexes, with or without solvate molecules. During the course of the kinetics studies on samples of $[Fe(dppen)_2Cl_2]\cdot n CHCl_3$ (**1**), it has been observed that the HS → LS relaxation is affected by the content (n) of solvate molecules in the crystal lattice of isostructural samples. More investigations on well-characterized crystals are required to reach a reliable insight into the crystal solvent effect. Work is in progress in this regard.

Concluding Comments

Light-induced spin-state conversion leading to long-lived metastable states (the LIESST effect) has been observed using ^{57}Fe Mössbauer spectroscopy for the $[Fe(dppen)_2X_2]\cdot 2S$ complexes, where X^- is either Cl^- or Br^- and the solvent molecule is either $CHCl_3$ or CH_2Cl_2. After photoexcitation at low temperatures, each complex persists in a metastable HS state. The slow rate of quantum mechanical tunneling from the metastable HS state to the stable LS state reflects the appreciable changes in Fe−ligand atom bond distances in converting from the HS $Fe^{II}P_4X_2$ complex to the LS complex. From the X-ray structures of $[Fe(dppen)_2Br_2]\cdot 2CHCl_3$ (**3**) at 149 and 193 K, below and above the spin-state interconversion, it is found that there is a relatively large change in the Fe−P bond length of 0.27 Å. This leads to thickness in the potential energy barrier that the complex has to tunnel through in the HS → LS relaxation.

The role that the solvent molecule plays in the HS → LS relaxation may not only be that of a space filler in the crystal, for the $X^- = Cl^-$, $S = CHCl_3$ complex **1** shows little cooperativity in the relaxation, whereas there is appreciable cooperativity seen through the sigmoidal relaxation decay curves for the other three complexes. Cooperativity is brought about by long-range elastic interactions[19,20] between the spin-state-changing complex molecules. The origin of such cooperative interactions is the drastic change of volume and shape of the complex molecules accompanying the spin-state transition. This causes "lattice pressure" ("image pressure") which is felt throughout the crystal, leading to cooperativity.

Acknowledgment. This work was supported by NSF Grant CHE-9420322 (D.N.H.). D.N.H. thanks the Humboldt Foundation for a Humboldt-Forschungspreis in 1993.

Supporting Information Available: Tables giving structure determination details, bond lengths, bond angles, anisotropic displacement coefficients, and hydrogen atom coordinates and isotropic displacement coefficients for the X-ray structures of $[Fe(dppen)_2Br_2]\cdot 2CHCl_3$ (**3**) at 149 and 193 K (13 pages). Ordering information is given on any current masthead page.

IC9700359